



OPEN

# PPAR $\alpha$ activation directly upregulates thrombomodulin in the diabetic retina

Akira Shiono<sup>1</sup>, Hiroki Sasaki<sup>1</sup>, Reio Sekine<sup>1</sup>, Yohei Abe<sup>2</sup>, Yoshihiro Matsumura<sup>2</sup>, Takeshi Inagaki<sup>3</sup>, Toshiya Tanaka<sup>4</sup>, Tatsuhiko Kodama<sup>4</sup>, Hiroyuki Aburatani<sup>5</sup>, Juro Sakai<sup>2,6</sup> & Hitoshi Takagi<sup>1</sup>✉

Two large clinical studies showed that fenofibrate, a commonly used peroxisome proliferator-activated receptor  $\alpha$  (PPAR $\alpha$ ) agonist, has protective effects against diabetic retinopathy. However, the underlying mechanism has not been clarified. We performed genome-wide analyses of gene expression and PPAR $\alpha$  binding sites in vascular endothelial cells treated with the selective PPAR $\alpha$  modulator pemafibrate and identified 221 target genes of PPAR $\alpha$  including *THBD*, which encodes thrombomodulin (TM). ChIP-qPCR and luciferase reporter analyses showed that PPAR $\alpha$  directly regulated *THBD* expression via binding to the promoter. In the rat diabetic retina, treatment with pemafibrate inhibited the expression of inflammatory molecules such as VCAM-1 and MCP1, and these effects were attenuated by intravitreal injection of small interfering RNA targeted to *THBD*. Furthermore, pemafibrate treatment inhibited diabetes-induced vascular leukostasis and leakage through the upregulation of *THBD*. Our results indicate that PPAR $\alpha$  activation inhibits inflammatory and vasopermeable responses in the diabetic retina through the upregulation of TM.

Diabetic retinopathy (DR) is the main cause of blindness among working-age adults, and the worldwide prevalence is approximately 35% in patients with diabetes<sup>1</sup>. DR is characterized by the combination of increased vessel permeability and progressive vascular occlusion. However, the molecular mechanisms underlying the pathways associated with DR have not been fully elucidated. Several biochemical mechanisms have been proposed to modulate the pathogenesis of DR through effects on cellular metabolism, signaling, and growth factors<sup>2</sup>. Implicated pathways include the accumulation of sorbitol and advanced glycation end-products, oxidative stress, protein kinase C activation, and upregulation of the renin-angiotensin system and vascular endothelial growth factor (VEGF). Among them, VEGF strongly promotes angiogenesis, a key mediator of the progression of DR. Inhibition of VEGF (e.g., anti-VEGF therapies) was shown to be effective in the management of DR in numerous studies<sup>3–7</sup>. However, some DR patients respond poorly or incompletely to anti-VEGF therapy. Accordingly, there is still substantial unmet medical need in patients with DR.

Peroxisome proliferator-activated receptor  $\alpha$  (PPAR $\alpha$ ) is a ligand-activated transcription factor that regulates lipid metabolism<sup>8</sup>. PPAR $\alpha$  is highly expressed in the liver and is also expressed in the retina<sup>9</sup>. Recently, two large, prospective clinical trials have demonstrated that fenofibrate, a canonical synthetic PPAR $\alpha$  agonist, has protective effects against DR in type 2 diabetes patients. The Fenofibrate Intervention in Event Lowering in Diabetes (FIELD) Study reported that fenofibrate therapy significantly reduced the cumulative need for laser therapy for DR<sup>10</sup>. The Action Control Cardiovascular Risk in Diabetes (ACCORD) Lipid Study of combination simvastatin and fenofibrate demonstrated a greater reduction in the progression of proliferative DR in type 2 diabetes patients compared with simvastatin alone<sup>11</sup>. Thus, PPAR $\alpha$  may be an emerging therapeutic option in DR.

Recently, it has been reported that PPAR $\alpha$  is downregulated by microRNA in the retina of diabetic animal models<sup>12</sup>. Previous studies showed that PPAR $\alpha$  exerts protective effects against endothelial dysfunction,

<sup>1</sup>Department of Ophthalmology, St. Marianna University of Medicine, 2-16-1 Sugao, Miyamae-ku, Kawasaki, Kanagawa, Japan. <sup>2</sup>Division of Metabolic Medicine, The University of Tokyo, RCAST, 4-6-1 Komaba, Meguro-ku, Tokyo, Japan. <sup>3</sup>Laboratory of Epigenetics and Metabolism, IMCR, Gunma University, 3-39-15 Showa-cho, Maebashi, Gunma, Japan. <sup>4</sup>Research Center for Advanced Science and Technology, The University of Tokyo, 4-6-1 Komaba, Meguro-ku, Tokyo, Japan. <sup>5</sup>Genome Science Division, The University of Tokyo, 4-6-1 Komaba, Meguro-ku, Tokyo, Japan. <sup>6</sup>Molecular Physiology and Metabolism Division, Tohoku University Graduate School of Medicine, 2-1 Seiryō-cho, Aoba, Sendai, Miyagi, Japan. ✉email: htakagimarianna@gmail.com

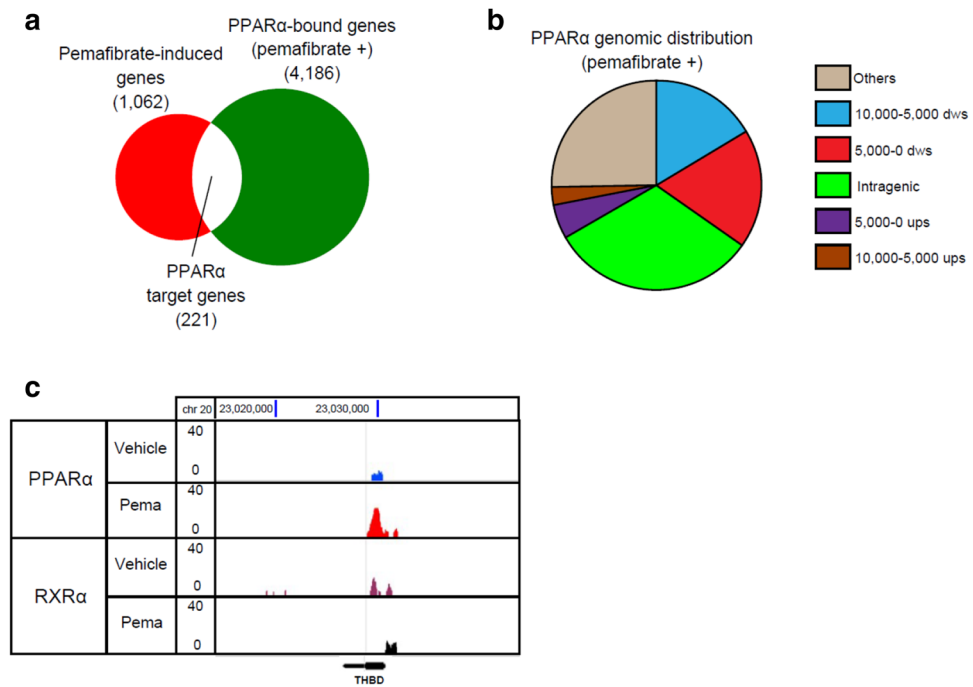


**Figure 1.** Genome-wide analysis of PPAR $\alpha$  binding sites in HUVECs. **(a)** Venn diagram representation of 1,062 pemaifibrate-induced genes ( $\geq 1.5$ -fold) and 4,186 PPAR $\alpha$ -bound genes in HUVECs treated with pemaifibrate (10  $\mu$ M). **(b)** Genome-wide distribution of PPAR $\alpha$  binding sites in pemaifibrate-treated HUVECs. Ups, upstream; dws, downstream. **(c)** Genome browser representation of PPAR $\alpha$  and RXR $\alpha$  binding on *THBD* in HUVECs treated with pemaifibrate (pema) or vehicle for 24 h.

neovascularization, vasoregression, and vascular hyperpermeability<sup>9,13–15</sup>. Another recent study has also found that important factors in DR such as VEGF and TNF $\alpha$  are downregulated by PPAR $\alpha$  activation in the retina of diabetic animal models<sup>16</sup>. However, the mechanisms by which PPAR $\alpha$  activation exerts protective effects against DR are not fully understood.

Fenofibrate, which has a long history of clinical use as a lipid-lowering drug, has poor PPAR subtype selectivity<sup>17</sup>. Fenofibrate treatment sometimes results in elevation of the transaminase, homocysteine, and creatine levels in patients. On the other hand, pemaifibrate, a novel selective PPAR $\alpha$  modulator, has greater PPAR $\alpha$  activation potency and higher subtype selectivity than fenofibrate<sup>18–20</sup>. Therefore, pemaifibrate may reduce inflammation and angiogenesis more effectively than fenofibrate in DR patients.

Thrombomodulin (TM) is a transmembrane protein expressed on the surface of endothelial cells and is encoded by the *THBD* gene<sup>21</sup>. TM converts thrombin to the anticoagulant form to reduce blood coagulation and inhibits inflammation in blood vessels<sup>22–26</sup>. Recently, recombinant TM has been developed and can potentially be used to treat patients with inflammatory and thrombotic diseases<sup>27,28</sup>.

In the current study, we performed genome-wide analyses of gene expression and PPAR $\alpha$  binding sites in vascular endothelial cells treated with pemaifibrate and found that PPAR $\alpha$  directly regulates the expression of *THBD* in endothelial cells. Furthermore, PPAR $\alpha$  activation inhibited retinal inflammation through the upregulation of TM in a rat model of DR. Thus, upregulation of TM by PPAR $\alpha$  activation can be a potential therapeutic strategy against DR.

## Results

**Genome-wide analysis of PPAR $\alpha$ -targeted genes in vascular endothelial cells.** To investigate the mechanism of the protective effects against DR by PPAR $\alpha$  activation, we performed DNA microarray analysis and ChIP-seq of PPAR $\alpha$  in HUVECs treated with pemaifibrate. Microarray analysis showed that pemaifibrate treatment for 24 h upregulated 1,062 genes ( $> 1.5$ -fold, Fig. 1a, pemaifibrate-induced genes) and downregulated 477 genes ( $> 1.5$ -fold) compared with DMSO treatment (control). Pemaifibrate-induced genes included known direct targets of PPAR $\alpha$  such as PDK4<sup>18</sup>. The top 50 upregulated and downregulated genes are listed in Tables 1 and 2, respectively.

In ChIP-seq analysis, peak calling by SICER identified 6,017 genomic regions as significant binding sites of PPAR $\alpha$  in pemaifibrate-treated HUVECs, and these binding sites were annotated to 4,186 genes (Fig. 1a, PPAR $\alpha$ -bound genes). The PPAR $\alpha$  genomic binding regions were localized mostly on intergenic regions (49%), and partly on proximal promoters (18%), and intragenic regions (31%) (Fig. 1b). Among PPAR $\alpha$ -bound genes, 221 overlapped with pemaifibrate-induced genes (Fig. 1a and Table 3). These target genes of PPAR $\alpha$  in HUVECs included *PDK4*, *ECH1*, and *ANGPTL4*, which are known metabolic genes induced by peroxisome proliferators<sup>18,29,30</sup>. We

LYVE1	ADAMTS1	LOC100288221	COL4A6	TCERG1L
GALNTL2	LOC727930	CCL23	FAHD2A///FAHD2B///LOC729234	RAB33A
THBD	TCEA3	MNS1	TSPAN7	CDKL1
PCDH17	DNAJC12	AK5	SLC25A30	BMP2
ASNS	EHD3	DPP4	TXNIP	TUBA4A
POSTN	HLX	AIFM3	LOC100509303///LOC100510086	LIFR
PLAT	HLA-DMA	ABHD14B	LOC389834	TFF3
KIAA1466	EDNRB	LIMCH1	C10orf116	MEF2C
SLC1A1	ADAMTS3	HCFC1R1	CASP12	MPZ
PDK4	PLS1	CPS1-IT	CH25H	LOC100270804

**Table 1.** List of upregulated genes.

SELE	VCAM1	IL8	KRT7	LOC100507507
CCL2	C1orf110	CLDN1	DKFZp547G183	PTX3
TGFB2	HSD17B2	GLIPR1	PMEP1	CYTL1
LYPD1	CXCL1	LRRC17	IL33	COL12A1
DKK1	GJA4	EVI2B	SYNGR3	SPSB1
GUCY1A3	RSPO3	ABCG2	TNKS2	TSPAN2
SEMA3G	GJA5	TOX	F2RL1	TNFRSF12A
CYP4X1	SERPINE2	C8orf48	PLAU	ENC1
DIRAS3	ANXA3	C6orf168	NMU	4-Mar
LOC100506828	PLA2G4C	TMSB15B	ZNF702P	ARSA

**Table 2.** List of downregulated genes.

also identified *THBD* encoding TM as a target gene of PPAR $\alpha$ . A genome browser shot showed pemaifibrate-dependent PPAR $\alpha$  binding near the transcription start site (TSS) of *THBD* (Fig. 1c).

We also performed ChIP-seq of retinoid X receptor  $\alpha$  (RXR $\alpha$ ), which is a heterodimer partner of PPAR $\alpha$ , and found RXR $\alpha$  binding near the TSS of *THBD* regardless of pemaifibrate treatment (Fig. 1c). Because TM is reported to inhibit inflammation in blood vessels<sup>23,26</sup>, we hypothesize that the upregulation of TM by PPAR $\alpha$  activation could inhibit the inflammatory response in the diabetic retina.

**PPAR $\alpha$  directly upregulates *THBD* expression.** A combination of DNA microarray and ChIP-seq analyses of HUVECs identified *THBD* as one of the target genes of PPAR $\alpha$ . To confirm this, we performed immunoblot analysis and showed that pemaifibrate treatment upregulated TM protein expression in HUVECs as well as HRMECs (Fig. 2a,b). Q-PCR analysis revealed that the upregulation of *THBD* by pemaifibrate was blunted when PPAR $\alpha$  was knocked down by small interfering RNA (siRNA) targeted to PPAR $\alpha$  in HUVECs and HRMECs (Fig. 2c,d). Thus, pemaifibrate-mediated induction of *THBD* is dependent on PPAR $\alpha$  in HUVECs and HRMECs. To determine whether PPAR $\alpha$  directly regulates *THBD* expression, we examined the physical and functional interactions of PPAR $\alpha$  with *THBD* in ChIP-qPCR and luciferase reporter analysis, respectively. ChIP-qPCR analysis confirmed PPAR $\alpha$  binding on the promoter region of *THBD* in HUVECs treated with pemaifibrate (Fig. 2e).

PPAR $\alpha$  preferentially binds DNA as a heterodimer to the PPAR-responsive element (PPRE), which is composed of two nuclear receptor consensus half-sites of AGGTCA organized as a direct repeat (direct repeat 1 [DR1])<sup>31</sup>. PPAR $\alpha$  forms heterodimers with RXR $\alpha$ , and the heterodimers bind the PPRE located in PPAR $\alpha$ -regulated genes. Scanning of the promoter sequences of human *THBD* identified two putative DR1 motifs (– 189 bp to 177 bp and – 1,135 bp to – 1,123 bp from the TSS) (Fig. 2f). The former motif is conserved in mouse and rat *Thbd* genes, while the latter is not (Fig. 2g). Accordingly, we generated a reporter plasmid containing the promoter of *THBD* (~ 1.3 kb) and performed luciferase reporter analysis (Fig. 2h). Because pemaifibrate affected the control reporter activities (i.e., renilla luciferase and  $\beta$ -gal) (data not shown), we used fenofibric acid as a PPAR $\alpha$  agonist in the luciferase reporter assay. HUVECs were transfected with the reporter plasmid together with expression plasmids of PPAR $\alpha$  and RXR $\alpha$  and then treated with fenofibric acid to determine PPAR $\alpha$ -mediated transactivation. Treatment with fenofibric acid increased the activity of the luciferase reporter containing the *THBD* promoter by threefold. Deletion of two putative DR1 motifs blunted the transactivation by fenofibric acid. Mutation in the DR1 motif at – 1,135 bp from the TSS alone had no effect on fenofibric acid-mediated transactivation, while mutation in the DR1 motif at – 189 bp from the TSS or mutations in both DR1 motifs abolished transactivation. These results indicate that PPAR $\alpha$  directly upregulates *THBD* expression in a ligand-dependent manner by binding to the DR1 motif at – 189 bp from the TSS in HUVECs.

NADK	NR4A2	ZNF827	DYNC1I1	TTLL11	TTC12	NOVA1	CALCOCO2
CTNNBIP1	METAP1D	PDLIM3	CUX1	PTGS1	VWA5A	RALGAPA1	MSI2
MTF1	FRZB	C5orf49	ATXN7L1	RC3H2	CD9	RAD51B	BCAS3
FOXJ3	MYO1B	FAM173B	TFEC	RALGPS1	ATF7IP	ZFP36L1	MED13
LEPR	CFLAR	ANKH	CFTR	ENG	TM7SF3	SPTLC2	ACE
PDE4B	RAPH1	RHOBTB3	GRM8	PTGES	ADAMTS20	FOXN3	MAP2K6
SLC35D1	HDAC4	LOC100289230	CALD1	FNBP1	ANO6	C15orf41	SDK2
AK5	CMTM7	ST8SIA4	RBM33	SURF6	GALNT6	TYRO3	RPTOR
PRKACB	STAB1	KLHL3	UBE3C	EHMT1	ACVR1B	MAPKBP1	SLC16A3
MAGI3	FHIT	ZNF346	CLN8	TUBBP5	ERBB3	TEX9	MEX3C
POU2F1	PTPRG	KIF13A	SLC25A37	IDI2-AS1	9-Mar	GTF2A2	LMAN1
DNM3	CD47	RNF144B	RBPMS	MSRB2	C12orf66	RORA	PIGN
FASLG	LRRC58	BAG6	NRG1	PDSS1	BEST3	DAPK2	CDH19
SEC16B	GOLGB1	TBC1D22B	ASPH	ARMC4	KCNMB4	EMP2	TMX3
DSTYK	KIAA1257	CEP57L1	UBE2W	BICC1	KITLG	EARS2	SBNO2
SLC45A3	ARHGEF26	TRAF3IP2	ZNF704	ANXA2P3	PLXNC1	NFATC3	ANGPTL4
MAPKAPK2	RARRES1	RNF217	RIMS2	SRGN	PARPBP	CDH13	ZNF441
SMYD2	MECOM	PDE7B	SMARCA2	CHST3	MORN3	ZFPM1	LPHN1
HLX	PLD1	MTRF1L	JAK2	RNLS	GOLGA3	SPG7	ZNF493
LYST	ZMAT3	ZDHC14	C9orf72	CTBP2	FLT1	TRPV2	PPP1R14A
LOC375196	ZCCHC4	WTAP	NFX1	STIM1	LINC00598	SHMT1	ECH1
EML6	PCDH7	AMZ1	PRSS3	CYP2R1	NUFIP1	SYNRG	PCED1A
NPAS2	LIMCH1	SDK1	LOC642236	CPT1A	SLC25A30	ARHGAP23	UBOX5
ST6GAL2	CEP135	GPNMB	C9orf85	ARRB1	PCDH17	EIF1	CDS2
TMEM37	ELOVL6	SKAP2	GABBR2	PCF11	UGGT2	DBF4B	PCSK2
CXCR4	INPP4B	PDK4	ZFP37	ZC3H12C	CLYBL	LOC100506325	TMPRSS15
THBD	WFDC8	ITSN1	UQCC	MRPL39	SGSM3	KLHL22	DYNLRB1
E2F1	BCAS4	DIP2A	TGM2	SYNJ1	DYNLRB1		

**Table 3.** List of overlapped genes.

**Pemafibrate inhibits TM-dependent retinal inflammation in diabetic rats.** Cell culture experiments showed that PPAR $\alpha$  directly upregulated TM, which has antiinflammatory effects. We hypothesized that PPAR $\alpha$  activation by pemafibrate could inhibit inflammation through upregulation of TM in the diabetic retina. To examine this, we first administered oral pemafibrate to rats via their feed and showed that pemafibrate (10 mg/kg or 30 mg/kg) significantly increased mRNA expression of PPAR $\alpha$  target genes such as *Pdk4* and *Thbd* in the retina (Fig. 3a,b). Next, we set up a TM knockdown system in the rat retina by intravitreal injection of siRNA. Intravitreal injection of 500 pmol of siRNA targeted to *Thbd* for 14 days successfully decreased the protein expression of TM (Fig. 3c). In the STZ-induced diabetic rat model, the protein levels of inflammatory molecules such as ICAM, MCP1, and VCAM-1 in the retina were elevated compared with the retinas of non-diabetic rats (Fig. 3d), as previously reported<sup>32,33</sup>. Oral intake of pemafibrate in STZ-induced diabetic rats markedly inhibited the elevation of inflammatory molecules, indicating that PPAR $\alpha$  activation inhibits inflammatory responses in the retinas of diabetic rats. Furthermore, knockdown of TM in diabetic rats attenuated the pemafibrate-mediated inhibition of elevation of inflammatory molecules. These results indicate that the inhibition of PPAR $\alpha$  activation by pemafibrate inhibits inflammation through the upregulation of TM in diabetic rat retinas.

**Pemafibrate inhibits TM-dependent retinal vascular leukostasis and leakage.** Vascular leukostasis and leakage increase cumulatively with the progression of DR<sup>34</sup>. To determine whether PPAR $\alpha$  activation inhibits vascular leukostasis and leakage in the retina, we examined them in diabetic rats treated with pemafibrate. FITC-labeled adherent leukocytes were not observed in control rats, while they were clearly observed in the retinal vasculature of untreated diabetic rats (Fig. 4a). Pemafibrate treatment significantly reduced the number of leukocytes in the rat retinas ( $p < 0.05$ ) (Fig. 4a,b), indicating that it inhibits vascular leukostasis in diabetic rats. TM knockdown by siRNA attenuated the pemafibrate-mediated reduction of leukocytes in the retinal vasculature of diabetic rats ( $p < 0.05$ ) (Fig. 4a,b), while control siRNA treatment did not, indicating that PPAR $\alpha$  activation by pemafibrate inhibits vascular leukostasis through TM in the retina of diabetic rats.

Next, we examined whether pemafibrate treatment reduces retinal vascular leakage in diabetic rats. The fluorescence intensity of FITC-dextran in the retinal vessels was significantly increased in diabetic rats compared with control rats ( $p < 0.05$ ), indicating increased vascular leakage in the former (Fig. 5a,b). Pemafibrate treatment significantly reduced the fluorescence intensity of FITC-dextran in diabetic rats ( $p < 0.05$ ) (Fig. 5a,b), indicating that PPAR $\alpha$  activation by pemafibrate inhibits vascular leakage. In addition, TM knockdown by siRNA attenuated pemafibrate-mediated inhibition of vascular leakage in diabetic rats ( $p < 0.05$ ) (Fig. 5a,b). These results revealed that PPAR $\alpha$  activation by pemafibrate inhibits retinal vascular leukostasis and leakage via TM in diabetic rats.

## Discussion

In the current study, we identified *THBD* encoding TM as one of the direct target genes of PPAR $\alpha$  in vascular endothelial cells. PPAR $\alpha$  activation by pemafibrate in a rat model of DR upregulated *THBD* and inhibited retinal inflammation and vascular leukostasis and leakage. To the best of our knowledge, this is the first report showing the novel molecular mechanism by which PPAR $\alpha$  activation protects against DR.

PPAR $\alpha$  is a ligand-activated transcription factor, and its target genes are involved in fatty acid metabolism in tissues with high oxidative rates such as the liver, heart, skeletal muscle, and kidney<sup>8,9</sup>. PPAR $\alpha$  is also expressed in other tissues and cells including the intestine, vascular endothelium, and immune cells<sup>15</sup>. Large clinical trials and several reports revealed that PPAR $\alpha$  activation by an agonist has protective effects against DR in type 2 diabetes patients<sup>10,11</sup>, although the mechanisms of action of the PPAR $\alpha$  agonist were unclear. Because DR is characterized by progressive loss of vascular cells and infiltration of inflammatory cells, we specifically focused on vascular endothelial cells and performed genome-wide analyses of PPAR $\alpha$  binding sites and gene expression using ChIP-seq analysis and DNA microarray. Our ChIP-seq analysis identified 6,017 genomic PPAR $\alpha$  binding sites, which were assigned to 4,186 proximal genes. Microarray analysis revealed 1,062 genes with expression levels upregulated by pemafibrate treatment in HUVECs.

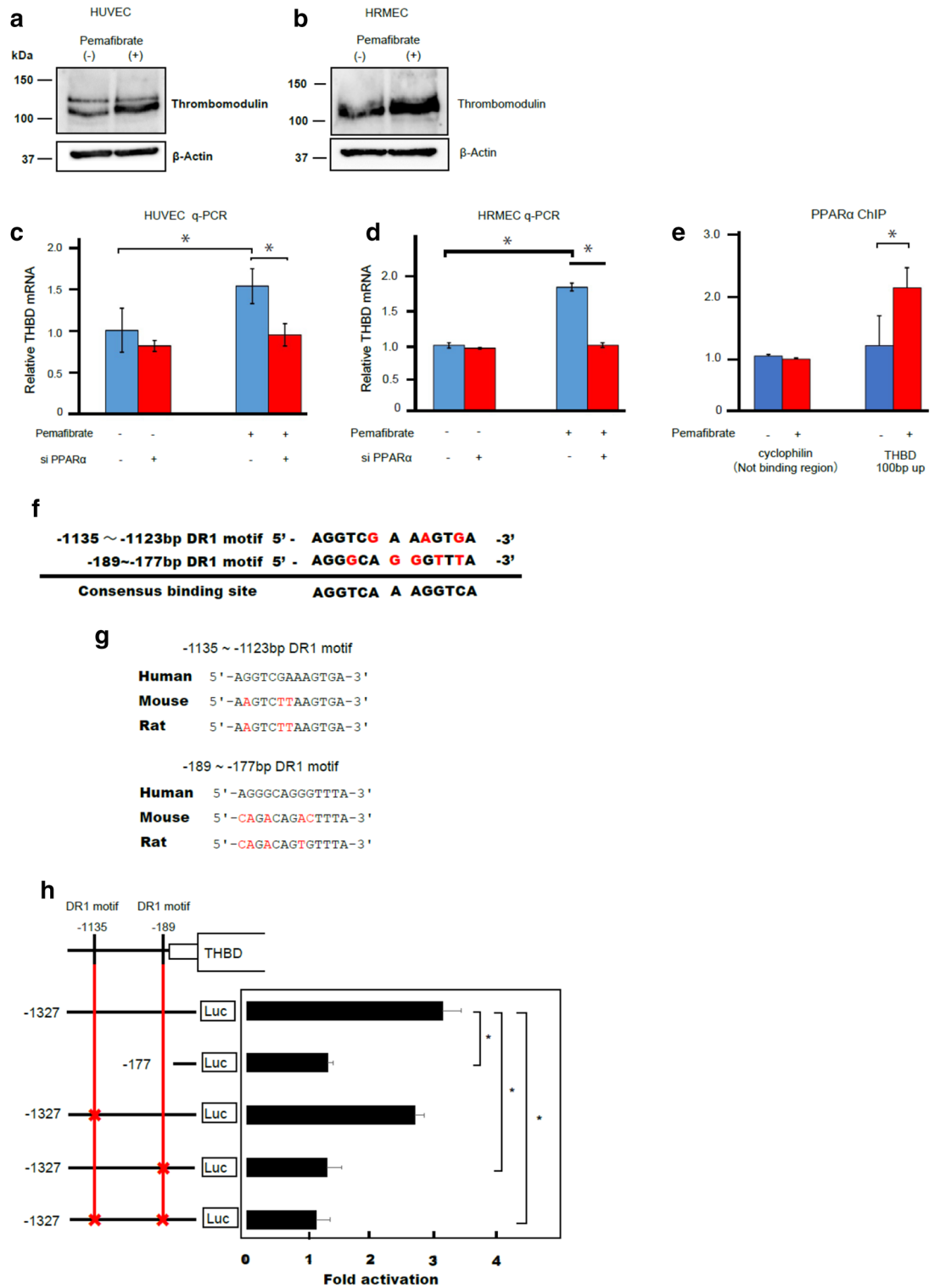
The majority of PPAR $\alpha$  binding sites identified by ChIP-seq were located at intragenic regions or 5' proximal regions (< 10 kb from the TSS) in HUVECs, consistent with previous ChIP-seq analysis in human hepatoma cells<sup>35</sup>. These results are in line with several studies showing that transcription factor binding sites are generally distributed around the TSS<sup>36,37</sup>. Among 4,186 genes annotated as bound by PPAR $\alpha$ , 221 including *THBD* were upregulated by pemafibrate treatment, indicating that these genes are direct PPAR $\alpha$  targets in HUVECs. However, pemafibrate treatment did not affect the expression of the majority of genes annotated as bound by PPAR $\alpha$ . Some PPAR $\alpha$  binding sites may participate in transcriptional regulation of distal genes or in other mechanisms such as noncoding RNA and DNA methylation. It is also possible that our ChIP-seq analysis contained false-positive signals due to the nonspecific binding of antibody. Therefore, the functional relevance of PPAR $\alpha$  binding sites needs to be elucidated further.

VEGF has been shown to be one of predominant factors regulating pathological conditions including chronic inflammation and resulting abnormal vasopermeable and angiogenic responses in DR. Our microarray analysis identified 1,062 upregulated and 477 downregulated genes in HUVECs treated with pemafibrate. VEGF mRNA was not altered in the present microarray analysis. Since it is possible that PPAR $\alpha$  has transcriptional and non-transcriptional roles in protection against DR, more detailed protein analyses are needed to confirm the direct effects of PPAR $\alpha$  activation on VEGF expression. In contrast, the inhibitory effects of PPAR $\alpha$  on VEGF expression were clearly demonstrated in in vivo settings. Chen et al. reported the inhibitory effects of fenofibrate on HIF-1 and VEGF expression in the whole retina in a type 1 diabetes rat model and mouse oxygen-induced retinal angiogenesis model<sup>38</sup>. Tomita et al. found that VEGF is suppressed by PPAR $\alpha$  activation, which inhibits HIF activity through serum FGF 12 induced and secreted in the liver<sup>39</sup>. Another study showed that PPAR $\alpha$  ligands may suppress angiogenesis indirectly by inhibiting tumor cell production of VEGF and FGF2 and by increasing thrombospondin-1<sup>40</sup>. Although we need further detailed protein expression analyses in in vitro studies, these data may indicate that PPAR $\alpha$  activation alone does not substantially affect VEGF expression, although it exerts obvious inhibitory effects through cross-reaction with other cytokines and organs. PPAR $\alpha$  effects on VEGF-induced intracellular signaling have not been reported and remain to be elucidated.

Among 221 direct PPAR $\alpha$  target genes, we focused on *THBD* that encodes TM. TM is an integral membrane protein expressed on the surface of endothelial cells and exerts antiinflammatory effects via several mechanisms<sup>22–26</sup>. TM inhibits inflammation through the activation of protease-activated receptor-1 (PAR-1) in the form of activated protein C (APC)<sup>23,24</sup>. Moreover, TM is a critical cofactor for thrombin-mediated activation of the thrombin-activatable fibrinolysis inhibitor (TAFI)<sup>21</sup>. The proinflammatory mediators are inactivated by TAFI<sup>25</sup>. TM, via thrombin-mediated activation of protein C and TAFI, provides protection against inflammation. Thrombin is an important inflammatory factor in retinal vascular diseases including DR<sup>41</sup>. It was reported that thrombin and prothrombin were increased in the vitreous of patients with proliferative DR compared with nondiabetic individuals<sup>42</sup>. Additionally, it was found that the lectin-like domain of TM sequesters inflammatory factors such as high-mobility group-B1 (HMGB-1) protein and lipopolysaccharide<sup>43,44</sup>. HMGB-1 promotes the process of cell apoptosis by activating the transcription factor nuclear factor- $\kappa$ B after binding to its receptors<sup>45,46</sup>. For these reasons, we hypothesized that PPAR $\alpha$  activation inhibited the retinal vascular damage caused by retinal inflammation and apoptosis via the regulation of TM.

In the transcriptional regulation of *THBD*, our studies revealed that PPAR $\alpha$  binds to the TSS upstream of *THBD* to activate gene expression. Furthermore, our luciferase reporter assay showed that the DR1 motif at 189 bp from the TSS is responsible for transactivation of the *THBD* promoter by PPAR $\alpha$ . Previous studies demonstrated that other transcriptional factors (e.g., Kruppel-like factor 2 and RXRs) also bind to this region to transactivate the *THBD* promoter<sup>47,48</sup>, suggesting the importance of this region for the activity of the *THBD* promoter in vascular endothelial cells.

We used the rat model of DR to show that pemafibrate treatment prevents the upregulation of inflammatory molecules as well as vascular leukostasis and leakage. It was reported that CCL2, VCAM-1, and ICAM-1 are key inflammatory molecules in the diabetic retina which lead to leukocyte adhesion and vascular leakage<sup>32,33</sup>. Inflammatory mediators such as thrombin and HMGB-1 induce these inflammatory molecules<sup>43,45,46</sup>, while TM has inhibitory effects on inflammatory molecules. Therefore, we performed TM knockdown experiments in diabetic rats to determine whether the antiinflammatory effect of pemafibrate is mediated via the action of TM. In vivo experiments demonstrated that the antiinflammatory effect of pemafibrate was canceled by intravitreal injection of *Thbd* siRNA. These results suggest that the upregulation of TM is one mechanism of the protective effects of PPAR $\alpha$  modulators (e.g., pemafibrate) against DR and that a modulator upregulating TM could be a



◀ **Figure 2.** PPAR $\alpha$  directly transactivates THBD expression. (a,b) Immunoblot analysis showing the expression of TM in HUVECs (a) and HRMECs (b) treated with pemaflibrate (10  $\mu$ M) or vehicle for 24 h. Expression of TM was increased by pemaflibrate treatment in both HUVECs and HRMECs. (c,d) HUVECs (c) and HRMECs (d) were transfected with siRNA targeted to human PPAR $\alpha$  (5 nM) or control siRNA and treated with pemaflibrate or vehicle for 24 h. *THBD* mRNA was measured using RT-qPCR. Cyclophilin mRNA was used as the invariant control. Knockdown of PPAR $\alpha$  canceled pemaflibrate-mediated upregulation of *THBD* in HUVECs and HRMECs. (e) PPAR $\alpha$  binding on the *THBD* promoter was evaluated by ChIP-qPCR. ChIP signals are presented as fold enrichment. Cyclophilin was used as a negative binding region. PPAR $\alpha$  was bound approximately 100 bp upstream from the TSS of *THBD*. (f) Alignment of promoter sequences of human *THBD*, mouse *Thbd*, and rat *Thbd* containing two putative DR1 motifs. The DR1 motifs at positions -1,135 to -1,123 bp and -189 to -177 bp of human *THBD* are conserved in mouse and rat *Thbd*. (g) Alignment of the two putative DR1 motifs in the human *THBD* promoter. At the consensus site, the consensus nucleotide found in the PPAR $\alpha$  binding sequences is represented by black letters. (h) Luciferase reporter analysis using the human *THBD* promoter. HUVECs were transfected with the luciferase reporter containing wild-type *THBD* promoter or indicated deletion and mutations in DR1 motifs together with PPAR $\alpha$  and RXR $\alpha$  expression plasmids. After transfection, HUVECs were treated with fenofibric acid for 24 h and subjected to the luciferase reporter assay. The luciferase activity with fenofibric acid was divided by the activity without fenofibric acid and is presented as fold activation. (Results are expressed as mean  $\pm$  SD of three independent experiments. \* $p$  < 0.05. Mann-Whitney  $U$  test).

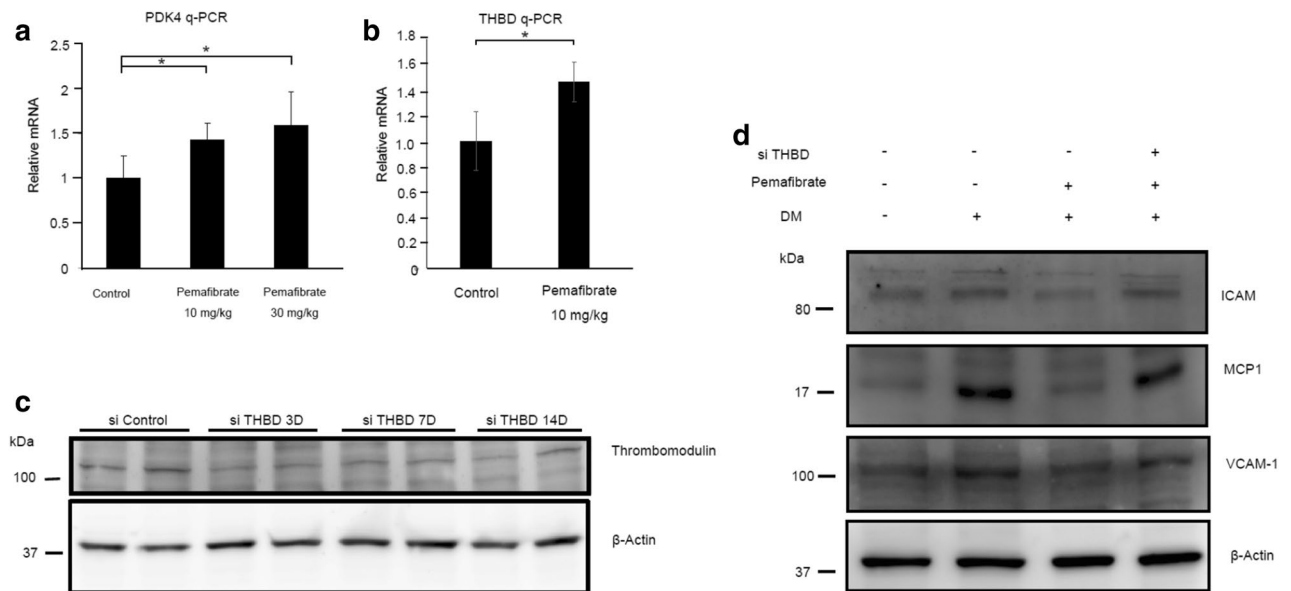


**Figure 3.** Pemaflibrate inhibits expression of inflammatory molecules by upregulating TM in the diabetic retina. (a) RT-qPCR analysis showing mRNA expression of *Pdk4* in rat retinas treated with the indicated doses of pemaflibrate. *Pdk4* is a known PPAR $\alpha$  target gene. Pemaflibrate treatment significantly upregulated *Pdk4* in the rat retina. (b) RT-qPCR showing mRNA expression of *Thbd* in rat retinas treated with pemaflibrate. Pemaflibrate significantly upregulated *Thbd* in the retina. (c) Immunoblot analysis showing expression of TM protein in the retinas of rats intravitreally injected with siRNA targeted to *Thbd* for 3, 7, and 14 days.  $\beta$ -Actin was used as a loading control. The intravitreal injection of siRNA reduced TM protein in the rat retina. (d) Immunoblot analysis showing expression of ICAM, MCP2, and VCAM-1 proteins in the retina of control and diabetic rats.  $\beta$ -Actin was used as a loading control. ICAM, MCP2, and VCAM-1 proteins were evaluated in the retinas of diabetic rats compared with control rats. Pemaflibrate treatment inhibited elevation of these proteins in the retina of diabetic rats. Knockdown of *Thbd* by siRNA canceled pemaflibrate-mediated inhibition of the elevation of these proteins. (Results are expressed as mean  $\pm$  SD of two independent experiments [a,b]. \* $p$  < 0.05. Mann-Whitney  $U$  test).

novel therapeutic option for DR treatment. Further studies will be required to elucidate other mechanisms by which PPAR $\alpha$  activation protects against DR.

## Methods

**Chemical reagents.** Pemaflibrate and fenofibric acid were kindly provided by Kowa Co., Ltd. (Nagoya, Japan).

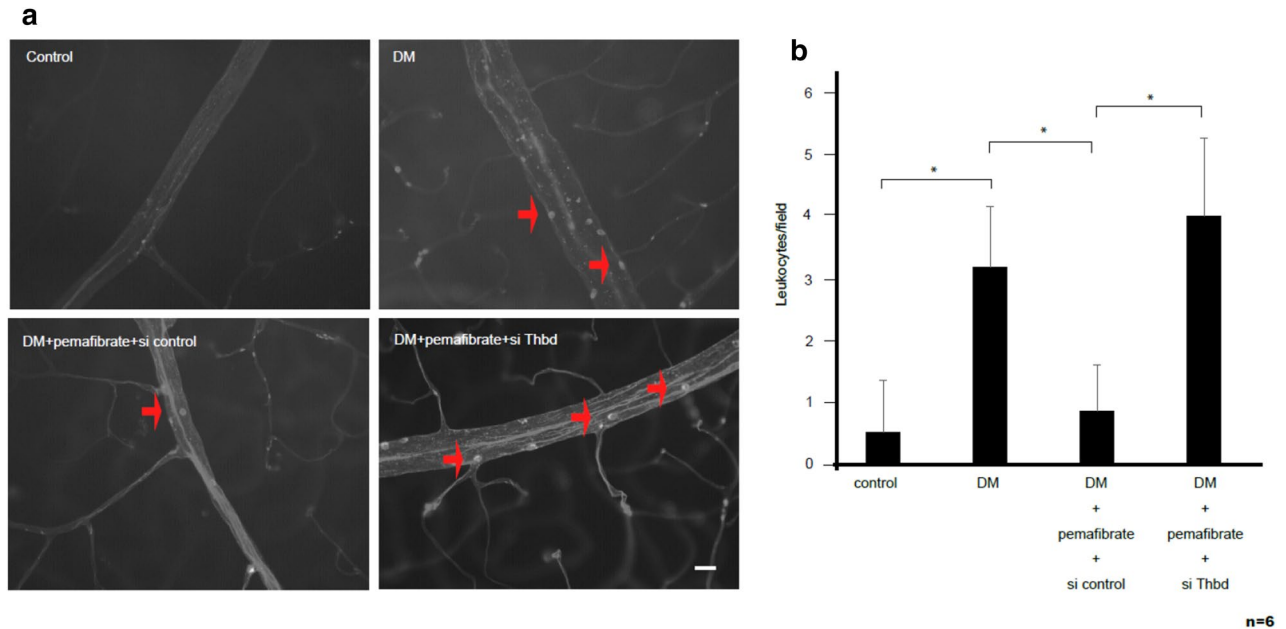


**Figure 4.** Pemaflibrate inhibits retinal vascular leukostasis by upregulating TM. **(a)** Fluorescence microscopy images showing retinal adherent vascular leukocytes in diabetic rats. STZ-induced diabetic rats were treated with pemaflibrate or vehicle and intravitreally injected with control siRNA or siRNA targeting *Thbd*. The retinal vascular adherent leukocytes were stained with FITC-conjugated concanavalin-A. Representative images of retinal flat mounts from nondiabetic rats (upper left), untreated diabetic rats (upper right), diabetic rats treated with pemaflibrate and control siRNA (lower left), and diabetic rats treated with pemaflibrate and si*Thbd* (lower right) are shown. Arrows indicate adherent leukocytes. Scale bar = 50  $\mu$ m. **(b)** Quantification of adherent leukocytes in retinal images (n = 6 per group). (Results are expressed as mean  $\pm$  SD. \*p < 0.05. Mann–Whitney U test).

**Cell culture.** Human umbilical vein endothelial cells (HUVECs) and human retinal microvascular endothelial cells (HRMECs) were purchased from Lonza (Walkersville, MD, USA) and cultured in EGM-2 MV medium (Lonza) containing 5% FBS at 37 °C in 5% CO<sub>2</sub>.

**siRNA-mediated knockdown of PPAR $\alpha$  and THBD.** Stealth small interfering RNA (siRNA) (5 nM) targeting human *THBD* mRNA (HSS110719, Invitrogen, Carlsbad, CA, USA) were transfected into HUVECs or HRMECs using RNAiMAX reagent (Invitrogen), and cells were harvested 24 h after transfection. Control siRNA (Med GC) was obtained from Invitrogen. For in vivo experiments, 500 pmol of siRNA targeting rat *Thbd* (RSS331106, Invitrogen) or control siRNA (sc-37007, Santa Cruz Biotechnology, Santa Cruz, CA, USA) was intravitreally injected into streptozotocin (STZ)-induced diabetic rats.

**DNA microarray analysis.** HUVECs were treated with 10  $\mu$ M of pemaflibrate or vehicle (DMSO) for 24 h, and total RNA was isolated using Isogen (Fujifilm Wako Chemicals, Osaka, Japan). Preparation of cRNA and hybridization of the probe arrays were performed according to the manufacturer's instructions (Affymetrix, Santa Clara, CA, USA)<sup>49</sup>. Affymetrix Genechip Human Genome U133 plus 2.0 arrays containing over 54,000 sets were used. Data analysis was performed using GeneSpring GX 12.5 (Agilent Technologies, Santa Clara, CA, USA).

**Chromatin immunoprecipitation.** HUVECs were treated with 10  $\mu$ M of pemaflibrate for 24 h and crosslinked with 1% formaldehyde for 10 min at room temperature. After neutralization by the addition of 0.2 M glycine, cells were harvested, resuspended in lysis buffer (13.6 mM Tris–HCl, 166.7 mM NaCl, 0.8% SDS, 1.2 mM EDTA, 0.9% Triton X-100; pH 8.0). Chromatin DNA was sonicated with Sonifier 250 (Branson, Danbury, CT, USA) (output 4, duty cycle 60%, 20 s  $\times$  6 times) to generate approximately 0.5-kb fragments. Chromatin immunoprecipitation (ChIP) was performed using the antibodies listed in Supplementary Table S1 prebound to Dynabeads Protein G (Life Technologies/Thermo Fisher Scientific, South San Francisco, CA, USA). ChIP DNA was purified with the QIAquick PCR Purification Kit (Qiagen, Germantown, MD, USA) and quantified using a Qubit Fluorometer and dsDNA HS assay Kit (Life Technologies/Thermo Fisher Scientific). ChIP sequencing (ChIP-seq) was performed with an Illumina/Solexa sequencer as previously described<sup>20–28,49–51</sup>.

**ChIP-qPCR analysis.** ChIP samples were analyzed by quantitative PCR using the gene-specific primers listed in Supplementary Table S2. ChIP signals were divided by no-antibody signals (input DNA) and presented as fold enrichment.



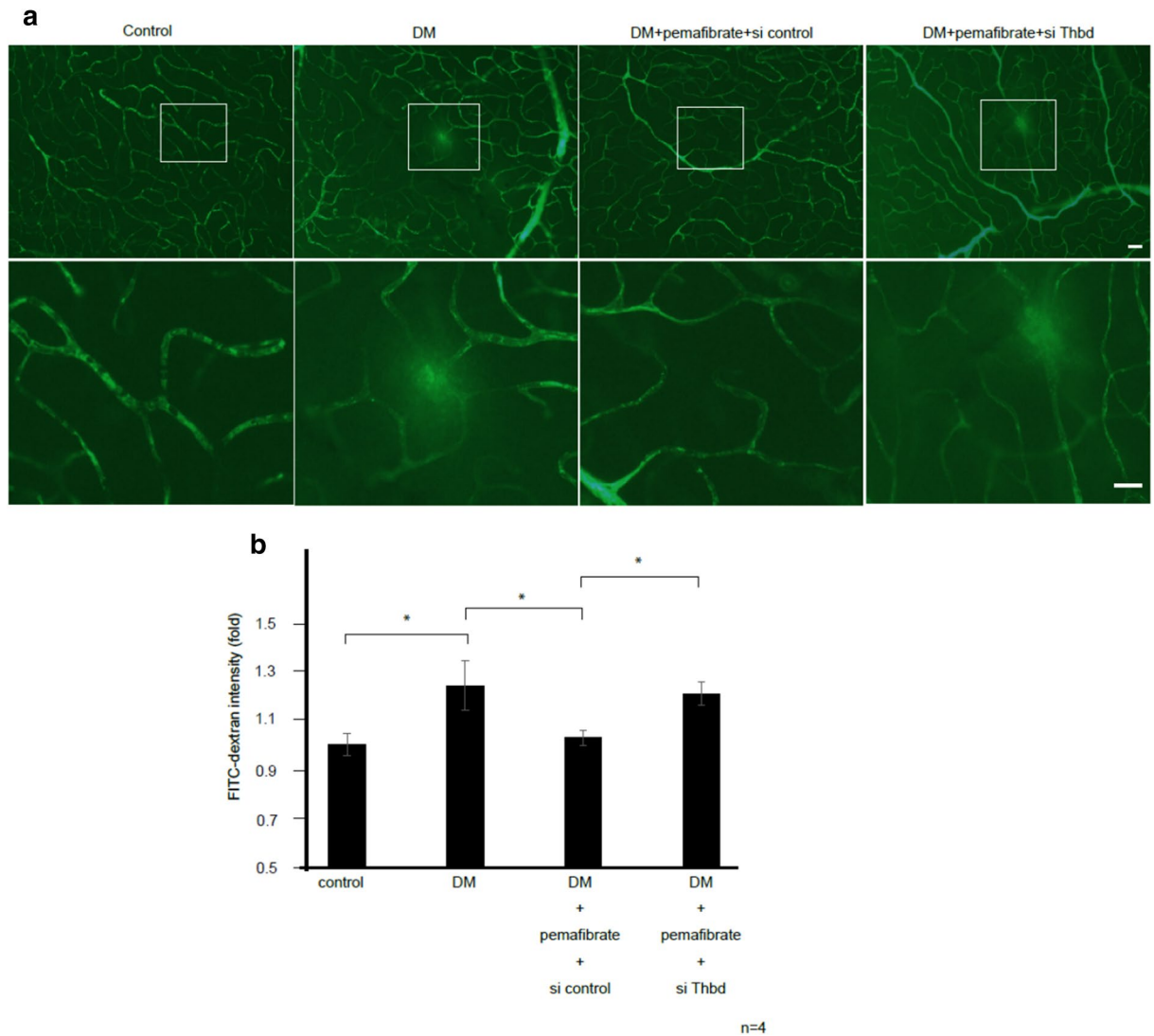


**Figure 5.** Pemafibrate inhibits retinal vascular leakage by upregulating TM. **(a)** Fluorescent images showing retinal vascular leakage in diabetic rats. STZ-induced diabetic rats were fed pemafibrate or vehicle. STZ-induced diabetic rats treated with pemafibrate or vehicle were then intravitreally injected with control siRNA or siRNA targeting *Thbd*. Vascular leakage was visualized by staining with FITC-dextran. Retinas were examined using fluorescence microscopy. Representative images of retinas from nondiabetic rats, untreated diabetic rats, diabetic rats treated with pemafibrate and control siRNA, and diabetic rats treated with pemafibrate and si*Thbd* are shown. The square areas in the top row are magnified and shown in the bottom row. Scale bar = 100  $\mu$ m. **(b)** Retinal permeability was quantified by measuring the fluorescence intensity of FITC-dextran in the images on the bottom row (n = 4 per group). (Results are expressed as mean  $\pm$  SD of three independent experiments. \* $p < 0.05$ . Mann-Whitney *U* test).

**Quantitative RT-PCR.** Total RNA was isolated using Isogen (Fujifilm Wako Chemicals) according to the manufacturer's protocol<sup>49</sup>. cDNA was synthesized from 1  $\mu$ g of total RNA using oligo-dT primers and SuperScript II reverse transcriptase (Life Technologies). Quantitative PCR was performed using an ABI PRISM 7900HT sequence detection system (Applied Biosystems, Foster City, CA, USA). *PPIB* or *ACTB* was used as an invariant control. A list of primers for quantitative RT-PCR used in this study is shown in Supplementary Table S3.

**Immunoblot analysis.** Protein samples obtained from HUVECs, HRMECs, or rat retinas were separated on 10% SDS-PAGE and electrophoretically transferred onto nitrocellulose membranes. The membranes were blocked with 5% skim milk in PBS containing 0.1% (v/v) Tween-20 for 1 h and incubated with primary antibody at 4  $^{\circ}$ C for 24 h. After washing, the membranes were incubated with secondary antibody conjugated with horseradish peroxidase at room temperature for 1 h. Immunoblots were visualized by chemiluminescence using Super Signal West Dura Extended Duration Substrate (Thermo Fisher Scientific), and luminescent images were

analyzed with an ImageQuant LAS 4000mini (GE Healthcare, Piscataway, NJ, USA). A list of primary antibodies used in this study is shown in Supplementary Table S1.

**Luciferase reporter assay.** The luciferase reporter assay was performed with the Beta-Glo assay system (Promega, Madison, WI, USA). HUVECs seeded on 24-well plates at 50% confluence in Opti-MEM (Life Technologies/Thermo Fisher Scientific) were transfected with 0.2  $\mu\text{g}$  of reporter plasmid. HUVECs were incubated for 24 h in normal growth medium and then treated with 100  $\mu\text{M}$  of fenofibric acid or vehicle (DMSO). Luciferase assays were performed 48 h after fenofibric acid treatment. Luciferase activity was normalized to the  $\beta$ -gal activity level.

**Type 1 diabetes rat model.** Type 1 diabetes was induced in male Wistar rats by an intraperitoneal injection of STZ (60 mg/kg). Briefly, 6 to 8 weeks after STZ injection, the rats were fed pemafibrate (10 mg/kg) for 2 weeks. Intravitreal injection of control or *Thbd* siRNA was performed 6 and 7 weeks after STZ injections. The rats were euthanized 8 weeks after STZ injection. Rats in which blood glucose levels were greater than 300 mg/dl at tissue harvesting were defined as diabetic and used for the experiments.

**Retinal vascular leukostasis assay.** The retinal vascular leukostasis assay was performed as described previously<sup>38</sup>. Briefly, rats were deeply anesthetized, and PBS was injected into the left ventricle. The anesthetized rats were perfused with PBS to remove nonadherent leukocytes in vessels. After injection of PBS, FITC-conjugated concanavalin-A (40  $\mu\text{g}/\text{ml}$ ) (Vector Laboratories, Burlingame, CA, USA) was injected into the left ventricle. The retinas were surgically isolated and then flat mounted. FITC-labeled adherent leukocytes in the vasculature were counted under a fluorescence microscope by an operator masked to treatment allocation.

**Measurement of vascular leakage in the retina.** Vascular leakage in the rat retinas was investigated using fluorescein angiography, as previously described<sup>52</sup>. Briefly, rats were deeply anesthetized, and FITC-dextran (Sigma-Aldrich, St. Louis, MO, USA) was injected into the left ventricle. After 5 min, the retinas were flat mounted and observed under a fluorescence microscope. Vascular leakage was quantitatively analyzed using Image J software by determining fluorescence intensities of FITC-dextran in the retina vessels.

**Study approval.** All animal protocols in this study were performed in accordance with the institutional guidelines and were approved by the St. Marianna University Graduate School of Medicine Institutional Animal Care and Use Committee.

## Data availability

All data generated or analyzed during this study are included in the published article (and its supplementary files).

Received: 11 October 2019; Accepted: 8 June 2020

Published online: 02 July 2020

## References

1. Yau, J. W. *et al.* Meta-analysis for eye disease (META-EYE) study group global prevalence and major risk factors of diabetic retinopathy. *Diabetes Care* **35**, 556–564 (2012).
2. Fong, D. S., Aiello, L. P., Ferris, F. L. III. & Kleon, R. Diabetic retinopathy. *Diabetes Care* **27**, 2540–2553 (2004).
3. Elman, M. J. *et al.* Expanded 2-year follow-up of ranibizumab plus prompt or deferred laser or triamcinolone plus prompt laser for diabetic macular edema. *Ophthalmology* **118**(4), 609–614 (2011).
4. Brown, D. M. *et al.* Long-term outcomes of ranibizumab therapy for diabetic macular edema: the 36-month results from two phase III trials: RISE and RIDE. *Ophthalmology* **120**(10), 2013–2022 (2013).
5. Schmidt-Erfurth, U. *et al.* Three-year outcomes of individualized ranibizumab treatment in patients with diabetic macular edema: the RESTORE Extension Study. *Ophthalmology* **121**(5), 1045–1053 (2014).
6. Korobelnik, J. F. *et al.* Intravitreal aflibercept for diabetic macular edema. *Ophthalmology* **121**(11), 2247–2254 (2014).
7. The Diabetic Retinopathy Clinical Research Network. Aflibercept, bevacizumab, or ranibizumab for diabetic macular edema. *N. Engl. J. Med.* **372**, 1193–1203 (2015).
8. Kersten, S. & Stienstra, R. The role and regulation of the peroxisome proliferator activated receptor alpha in human liver. *Biochimie* **136**, 75–84 (2017).
9. Hiukka, A., Maranghi, M., Matikainen, N. & Taskinen, M. R. PPARalpha: an emerging therapeutic target in diabetic microvascular damage. *Nat. Rev. Endocrinol.* **6**(8), 454–463 (2010).
10. Keech, A. C. *et al.* Effect of fenofibrate on the need for laser treatment for diabetic retinopathy (FIELD study): a randomized controlled trial. *Lancet* **370**, 1687–1697 (2007).
11. Chen, E. Y. *et al.* Effects of medical therapies on retinopathy progression in type 2 diabetes. *N. Engl. J. Med.* **363**, 233–244 (2010).
12. Chen, Q. *et al.* Pathogenic role of microRNA-21 in diabetic retinopathy through downregulation of PPAR $\alpha$ . *Diabetes* **66**(6), 1671–1682 (2017).
13. Bordet, R. *et al.* PPAR: a new pharmacological target for neuroprotection in stroke and neurodegenerative disease. *Biochem. Soc. Trans.* **34**, 1341–1346 (2006).
14. Mysiorek, C. *et al.* Peroxisome-proliferator-activated receptor-alpha activation protects brain capillary endothelial cells from oxygen-glucose deprivation-induced hyperpermeability in the blood-brain barrier. *Curr. Neurovasc. Res.* **6**, 181–193 (2009).
15. Lefebvre, P., Chinetti, G., Fruchart, J. C. & Staels, B. Sorting out the roles of PPAR alpha in energy metabolism and vascular homeostasis. *J. Clin. Invest.* **116**, 571–580 (2006).
16. Deng, G. *et al.* Therapeutic effects of a novel agonist of peroxisome proliferator-activated receptor alpha for the treatment of diabetic retinopathy. *Invest. Ophthalmol. Vis. Sci.* **58**(12), 5030–5042 (2017).
17. Knopp, R. H. *et al.* Effect of fenofibrate treatment on plasma lipoprotein lipids, high-density lipoprotein cholesterol subfractions, and apolipoproteins B, AI, AII, and E. *Am. J. Med.* **83**(58), 75–84 (1987).

18. Raza-Iqbal, S. *et al.* Transcriptome analysis of K-877 (a novel selective PPARalpha modulator (SPPARalpha))-regulated gene in primary human hepatocytes and mouse liver. *J. Atheroscler. Thromb.* **22**, 754–772 (2015).
19. Takei, K. *et al.* Effects of K-877, a novel selective PPARalpha modulator, on small intestine contribute to the amelioration of hyperlipidemia in low-density lipoprotein receptor knockout mice. *J. Pharmacol. Sci.* **133**(4), 214–222 (2017).
20. Honda, Y. *et al.* Pemafibrate, a novel selective peroxisome proliferator-activated receptor alpha modulator, improves the pathogenesis in a rodent model of nonalcoholic steatohepatitis. *Sci. Rep.* **14**(7), 42477 (2017).
21. Sadler, J. E. Thrombomodulin structure and function. *Thromb. Haemost.* **78**(1), 392–395 (1997).
22. Beffa, M. C., Burke, B. & Haudenschild, C. C. Prevention of thrombomodulin antigen on vascular and extravascular surfaces. *J. Histochem. Cytochem.* **25**(11), 1267–1276 (1987).
23. Riewald, M., Petrovan, R. J., Donner, A. & Ruf, W. Activated protein C signals through the thrombin receptor PAR1 in endothelial cells. *J. Endotoxin. Res.* **9**(5), 317–321 (2003).
24. Cheng, T. *et al.* Activated protein C blocks p53-mediated apoptosis in ischemic human endothelium and is neuroprotective. *Nat. Med.* **9**(3), 338–342 (2003).
25. Bajzar, L., Manuel, R. & Nesheim, M. E. Purification and characterization of TAFI, a thrombin-activated fibrinolysis inhibitor. *J. Biol. Chem.* **270**(24), 14477–14484 (1995).
26. Myles, T. *et al.* Thrombin activatable fibrinolysis inhibitor, a potential regulator of vascular inflammation. *J. Biol. Chem.* **278**(51), 51059–51067 (2003).
27. Inoue, Y., Matsunawa, M., Sano, F. & Miura, I. Efficacy of recombinant human soluble thrombomodulin in treating disseminated intravascular coagulation complicating allogeneic hematopoietic stem cell transplantation. *Acta Haematol.* **140**(2), 121–127 (2018).
28. Yasuda, N. *et al.* The efficacy and safety of antithrombin and recombinant human thrombomodulin combination therapy in patients with severe sepsis and disseminated intravascular coagulation. *J. Crit. Care* **36**, 29–34 (2016).
29. Lu, Y. F. *et al.* Icaria is a PPAR activator inducing lipid metabolic gene expression in mice. *Molecules* **19**(11), 18179–18191 (2014).
30. Inoue, Y. *et al.* Cross-enhancement of ANGPTL4 transcription by HIF1 alpha and PPAR beta/delta is the result of the conformational proximity of two response elements. *Genome Biol.* **15**(4), R63 (2014).
31. Schoonjans, K. *et al.* PPARalpha and PPARgamma activators direct a distinct tissue-specific transcriptional response via a PPRE in the lipoprotein lipase gene. *EMBO J.* **15**(19), 5336–5348 (1996).
32. Yoshida, S., Yoshida, A., Ishibashi, T., Elner, S. G. & Elner, V. M. Role of MCP-1 and MIP-1 alpha in retinal neovascularization during postischemic inflammation in a mouse model of retinal neovascularization. *J. Leukoc. Biol.* **73**, 137–144 (2003).
33. Miyamoto, K. *et al.* Prevention of leukostasis and vascular leakage in streptozotocin-induced diabetic retinopathy via intercellular adhesion molecule-1 inhibition. *Proc. Natl. Acad. Sci. USA* **96**(19), 10836–10841 (1999).
34. Schmidt-Erfurth, U. *et al.* Guidelines for the management of diabetic macular edema by the European Society of Retina Specialists (EURETINA). *Ophthalmologica* **237**(4), 185–222 (2017).
35. van der Meer, D. L. *et al.* Profiling of promoter occupancy by PPARalpha in human hepatoma cells via ChIP-chip analysis. *Nucleic Acids Res.* **38**(39), 2839–2850 (2010).
36. Hamza, M. S. *et al.* De-novo identification of PPARgamma/RXR binding sites and direct targets during adipogenesis. *PLoS ONE* **4**(3), e4907 (2009).
37. Zeller, K. I. *et al.* Global mapping of c-Myc binding sites and target gene networks in human B cells. *Proc. Natl. Acad. Sci. USA* **103**(47), 17834–17839 (2006).
38. Chen, Y. *et al.* Therapeutic effects of PPAR agonist on diabetic retinopathy in type 1 diabetes models. *Diabetes* **62**(1), 261–272 (2013).
39. Tomita, Y. *et al.* Pemafibrate prevents retinal pathological neovascularization by increasing FGF21 level in a murine oxygen-induced retinopathy model. *Int. J. Mol. Sci.* **20**(23), 5878 (2019).
40. Panigrahy, D. *et al.* PPARalpha agonist fenofibrate suppresses tumor growth through direct and indirect angiogenesis inhibition. *Proc. Natl. Acad. Sci. USA* **105**(3), 985–990 (2008).
41. Murugesan, N., Ustunkaya, T. & Feener, E. P. Thrombosis and hemorrhage in diabetic retinopathy: a perspective from an inflammatory standpoint. *Semin. Thromb. Hemost.* **41**(6), 659–664 (2015).
42. Bastiaans, J. *et al.* The role of thrombin in proliferative vitreoretinopathy. *Invest. Ophthalmol. Vis. Sci.* **55**(7), 4659–4666 (2014).
43. Abeyama, K. *et al.* The N-terminal domain of thrombomodulin sequesters high-mobility group-B1 protein, a novel anti-inflammatory mechanism. *J. Clin. Invest.* **115**(5), 1267–1274 (2005).
44. Shi, C. S. *et al.* Lectin-like domain of thrombomodulin binds to its specific ligand Lewis Y antigen and neutralizes lipopolysaccharide-induced inflammatory response. *Blood* **112**(9), 3661–3670 (2008).
45. Yang, H., Wang, H., Chavan, S. S. & Andersson, U. High mobility group box protein 1 (HMGB1): the prototypical endogenous danger molecule. *Mol. Med.* **21**, 6–12 (2015).
46. Palumbo, R. *et al.* Cells migrating to sites of tissue damage in response to the danger signal HMGB1 require NF-kappaB activation. *J. Cell. Biol.* **179**, 33–40 (2007).
47. Lin, Z. *et al.* Kruppel-like factor 2 (KLF-2) regulates endothelial thrombotic function. *Circ. Res.* **96**(5), e48–57 (2005).
48. Horie, S. *et al.* Acceleration of thrombomodulin gene transcription by retinoid acid: retinoid acid receptors and Sp1 regulate the promoter activity through interactions with two different sequences in the 5'-flanking region of human gene. *J. Biol. Chem.* **276**(4), 2440–2450 (2000).
49. Abe, Y. *et al.* JMJD1A is a single-sensing scaffold that regulates acute chromatin dynamics via SWI/SNF association for thermogenesis. *Nat. Commun.* **7**(6), 7052. <https://doi.org/10.1038/ncomms8052> (2015).
50. Okamura, M. *et al.* COUP-TFII acts downstream of Wnt/beta-catenin signal to silence PPARgamma gene expression and repress adipogenesis. *Proc. Natl. Acad. Sci. USA* **106**(14), 5819–5824 (2009).
51. Wakabayashi, K. *et al.* The peroxisome proliferator-activated receptor gamma/retinoid X receptor alpha heterodimer targets the histone modification enzyme PR-set7/Setd8 gene and regulates adipogenesis through a positive feedback loop. *Mol. Cell. Biol.* **29**(13), 3544–3555 (2009).
52. Lee, Y. J. *et al.* Essential role of transglutaminase 2 in vascular endothelial growth factor-induced vascular leakage in the retina of diabetic mice. *Diabetes* **65**(8), 2414–2428 (2016).

## Acknowledgements

We thank Dr. Jiro Kogo, Dr. Yasushi Kitaoka, and Yukari Hari for helpful discussions. Dr. Hitoshi Takagi is the guarantor of this work and as such had full access to all the data in the study and takes responsibility for the integrity of the data and the accuracy of the data analysis.

## Author contributions

Y.M., T.I., T.T., T.K., J.S., and H.T. conceived of and planned the experiments. A.S., R.S., H.S., Y.A., and Y.M. performed the experiments. A.S., Y.M., and H.T. wrote the manuscript. T.I., T.T., T.K., H.A., and J.S. helped supervise the project.

### Competing interests

The authors declare no competing interests.

### Additional information

**Supplementary information** is available for this paper at <https://doi.org/10.1038/s41598-020-67579-1>.

**Correspondence** and requests for materials should be addressed to H.T.

**Reprints and permissions information** is available at [www.nature.com/reprints](http://www.nature.com/reprints).

**Publisher's note** Springer Nature remains neutral with regard to jurisdictional claims in published maps and institutional affiliations.



**Open Access** This article is licensed under a Creative Commons Attribution 4.0 International License, which permits use, sharing, adaptation, distribution and reproduction in any medium or format, as long as you give appropriate credit to the original author(s) and the source, provide a link to the Creative Commons license, and indicate if changes were made. The images or other third party material in this article are included in the article's Creative Commons license, unless indicated otherwise in a credit line to the material. If material is not included in the article's Creative Commons license and your intended use is not permitted by statutory regulation or exceeds the permitted use, you will need to obtain permission directly from the copyright holder. To view a copy of this license, visit <http://creativecommons.org/licenses/by/4.0/>.

© The Author(s) 2020